Numer. Math. Theor. Meth. Appl.
doi: 10.4208/nmtma.OA-2021-0065

Vol. **15**, No. 1, pp. 125-140
February 2022

An Efficient Variational Model for Multiplicative Noise Removal

Min Liu[1] and Xiliang Lu[1,2,*]

[1] *School of Mathematics and Statistics, Wuhan University, Wuhan 430072, China*
[2] *Hubei Key Laboratory of Computational Science, Wuhan University, Wuhan 430072, China*

Received 25 April 2021; Accepted (in revised version) 19 October 2021

Abstract. In this paper, an efficient variational model for multiplicative noise removal is proposed. By using a MAP estimator, Aubert and Aujol [SIAM J. Appl. Math., 68(2008), pp. 925-946] derived a nonconvex cost functional. With logarithmic transformation, we transform the image into a logarithmic domain which makes the fidelity convex in the transform domain. Considering the TV regularization term in logarithmic domain may cause oversmoothness numerically, we propose the TV regularization directly in the original image domain, which preserves more details of images. An alternative minimization algorithm is applied to solve the optimization problem. The z-subproblem can be solved by a closed formula, which makes the method very efficient. The convergence of the algorithm is discussed. The numerical experiments show the efficiency of the proposed model and algorithm.

AMS subject classifications: 65M10, 78A48

Key words: Multiplicative noise, variational model, alternating direction minimization.

1. Introduction

Image recovery encompasses the large body of inverse problems, in which a multidimensional signal u is inferred from the observation data f, consisting of signals physically or mathematically related to it. The objective is to recover the original image from the observation of a contaminated image. The original image can be degraded by different mathematical methods. The most famous variational model for additive noise removal is Rudin-Osher-Fatemi (ROF) model [24]. Many other variational methods are also proposed, for instance [9, 11, 13, 16, 21, 27]. The ROF model introduced

*Corresponding author. *Email addresses:* `mliuf@whu.edu.cn` (M. Liu), `xllv.math@whu.edu.cn` (X. Lu)

total variational minimization to image processing, which can preserve the edges well. The additive noise model is generated from the model $f = u + \eta$, where f, u and η are observed image, true image and the additive noise, respectively. The ROF model defined the solution as follows:

$$u = \underset{u \in BV(\Omega)}{\operatorname{argmin}} \; |u|_{BV} + \frac{\lambda}{2}\|f - u\|_{L^2}^2$$

for a regularization parameter $\lambda > 0$, where $BV(\Omega)$ denotes the space of function with bounded variation on Ω, equipped with the BV seminorm which is formally given by

$$|u|_{BV} = \int_\omega |\nabla u|,$$

also noted as the total variation (TV) of u.

Multiplicative noise, also known as speckle noise, has not been discussed thoroughly when compared with additive noise. Multiplicative noise occurs in many areas, such as magnetic field inhomogeneity in MRI [2], ultrasound images [17], synthetic aperture radar (SAR) images [19], etc. We consider the problem of recovering the original image u, which is corrupted by multiplicative noise η. i.e., $f = u\eta$ with assumption $f > 0$. One often assume that the noise η follows Gamma distribution, which commonly occurs in SAR. The probability density function of η is denoted as P_η,

$$P_\eta(x, \theta, K) = \frac{1}{\theta^K \Gamma(K)} x^{K-1} e^{-\frac{x}{\theta}}, \tag{1.1}$$

where Γ is Gamma function, and θ and K denote the scale and shape, respectively. The mean of η is $K\theta$ and the variance of η is $K\theta^2$.

The total variation approach to multiplicative noise model was proposed by Rudin *et al.* [23], in which the multiplicative noise is assumed to Gaussian distribution. Although [23] can restore images well, the Gaussian multiplicative noise is not common in real applications. For the Gamma distributed multiplicative noise, Aubert and Aujol [1] proposed a variational model based on the maximum a posteriori (MAP) estimator as follows, which is referred to as AA model

$$\inf_{u \in S(\Omega)} \int_\Omega \left(\log u + \frac{f}{u} \right) dx + \lambda \int_\Omega |Du|. \tag{1.2}$$

The second term is the TV regularization term and λ is regularization parameter to trade-off. Although the fidelity term in (1.2) is not convex, they also give the existence of minimizer and proved the uniqueness with a sufficient condition. The nonconvex fidelity raises the difficult to achieve the global optimal, and the numerical result often dependent on the initial guess. Based on AA model, spatially varying regularization parameter is discussed in [20] to get more texture details. By the logarithmic transformation, $f = u\eta$ turns to $\log f = \log u + \log \eta$, which can be treated as additive noise. Relaxed inverse scale space (RISS) flow is used to solve u in [25] and we denote it as SO model. Huang *et al.* [18] use the logarithmic transformation and discuss the image in the logarithmic domain. An auxiliary variable and a quadratic penalty term also introduced. An alternating minimization algorithm and convergence are developed. We name it as HM model. Both SO and HM discussed images in the logarithmic domain, which are convex models, but may cause oversmooth. Steidl and Teuber [26] introduced the I-divergence as the fidelity term and the TV or the nonlocal means as the regularization term. Also, [26] proves the relation between the SO model and the I-divergence model. In [28], Yun and Woo propose the mth root transformation to deal with the nonconvexity of AA model. By rewriting a blur and multiplicative noise equation such that both the image variable and the noise variable are decoupled, [30] proposed a new optimization model for multiplicative noise and blur removal. Dictionary learning and sparse representation methods also been developed for multiplicative noise removal, see [8].

In this paper, we focus on the restoration of images that are corrupted by multiplicative noise which is supposed to follow the Gamma distribution. As in (1.2), we denote $z=\log u$, i.e., $u=e^z$. To preserve the edges and overcome the oversmooth in the logarithmic domain, we adopt the TV regularization in the original image domain. Furthermore we add a penalty term $\|u-e^z\|_2^2$ to keep the consistence between image domain and the logarithmic domain. Alternating minimization algorithm is discussed to solve the proposed model. In each iteration, we observe that one can solve e^z in a closed formula, which is very efficient.

The rest of this paper is organized as follows. In Section 2 we proposes the variational model and an alternating iterative algorithm to solve it. The convergence analysis is given in Section 3. In Section 4 numerical experiments are presented to show the efficiency of the proposed model.

2. The variational model and the alternative direction algorithm

For simplicity we consider an $n\times n$ image. Let $z=\log u$, that is $u=e^z$. The data fitting term is derived from the statistical perspective of Bayesian formulation in [1], which can be written as $\sum_{i=1}^{n^2}([z]_i+[f]_ie^{-[z]_i})$. Then combining with a TV-regularizer in image domain as well as a penalty term for the consistence of the image domain and the logarithmic domain, we can propose the variational model as follows:

$$\min_{z,u\in\Omega} E(z,u)=\sum_{i=1}^{n^2}\Big([z]_i+[f]_ie^{-[z]_i}\Big)+\alpha_1\|u-e^z\|_2^2+\alpha_2\|u\|_{TV}, \tag{2.1}$$

where $f\in\mathbb{R}^{n^2}$ is a given vector with positive components, α_1 and α_2 are two positive constants to balance the three terms. The convex set Ω imposes the box constraints to image u, which will be discussed in Section 3. Then we describe an alternative minimization algorithm to solve the proposed model (2.1).

Algorithm 2.1 involves z-subproblem (2.2) and u-subproblem (2.3). Now we discuss how to solve (2.2) and (2.3) in details.

Algorithm 2.1

1: Initialize $u^0 = f$;
2: Calculate $z^{(k)}$, $u^{(k)}$ from

$$z^{(k)} = \underset{z}{\operatorname{argmin}} \sum_{i=1}^{n^2} \left([z]_i + [f]_i e^{-[z]_i}\right) + \alpha_1 \|u^{(k-1)} - e^z\|_2^2, \tag{2.2}$$

$$u^{(k)} = \underset{u\in\Omega}{\operatorname{argmin}}\, \alpha_1 \|u - e^{z^{(k)}}\|^2 + \alpha_2 \|u\|_{TV}. \tag{2.3}$$

3: Stop or set $k = k + 1$ and go to Step 2
4: Output u^k.

For the z-subproblem, the necessary condition to (2.2) is the following nonlinear system:

$$1 - [f]_i e^{-[z]_i} + 2\alpha_1 \left(e^{[z]_i} - [u^{(k-1)}]_i\right) e^{[z]_i} = 0, \quad i = 1, \ldots, n^2. \tag{2.4}$$

Multiplying $e^{[z]_i}$ in the both sides, (2.4) can be rewritten as

$$e^{[z]_i} - [f]_i + 2\alpha_1 e^{2[z]_i} \left(e^{[z]_i} - [u^{(k-1)}]_i\right) = 0, \quad i = 1, \ldots, n^2,$$

which is a cubic equation

$$2\alpha_1 e^{3[z]_i} - 2\alpha_1 [u^{(k-1)}]_i e^{2[z]_i} + e^{[z]_i} - [f]_i = 0 \tag{2.5}$$

and has a closed form solution. We can then compute $e^{[z]_i}$ directly and use it in the u-subproblem.

The u-subproblem is a TV denoising with box constraint model

$$\min_{u\in\Omega} \alpha_1 \left\|u - e^{z^{(k)}}\right\|_2^2 + \alpha_2 \|u\|_{TV}. \tag{2.6}$$

The TV denoising model can be efficiently solved by various methods, such as split-Bregman algorithm [14], Chambolle' semi-implicit gradient decent method [4], semismooth Newton's method [15], alternating direction method of multipliers (ADMM) [12] and the primal-dual hybrid gradient algorithm [5]. We will use ADMM for solving u-subproblem, which can handle the box constraint easily. Let $\mu = 2\alpha_1/\alpha_2$ and $g = e^{z^k}$, then by introducing auxiliary variables x and y, problem (2.6) can be formulated as

$$\min_{x\in\Omega, u, y} \left\{ \frac{\mu}{2} \|u - g\|_2^2 + \sum_i \|y_i\|_2 : y_i = D_i u,\ i = 1, \ldots, n^2;\ u = x \right\}, \tag{2.7}$$

where

$$D_i u := \left(\left(D^{(1)} u\right)_i, \left(D^{(2)} u\right)_i\right)^\top \in \mathbb{R}^2, \quad i = 1, \ldots, n^2$$

and

$$\left(D^{(1)}u\right)_i := \begin{cases} u_{i+n} - u_i, & \text{if} \quad 1 \le i \le n(n-1), \\ u_{\bmod (i,n)} - u_i, & \text{otherwise}, \end{cases}$$
$$\left(D^{(2)}u\right)_i := \begin{cases} u_{i+1} - u_i, & \text{if} \quad \bmod (i,n) \neq 0, \\ u_{i-n+1} - u_i, & \text{otherwise}. \end{cases}$$

The augmented Lagrangian $\mathcal{L}(u, y, x; \lambda, \xi)$ is given by

$$\begin{aligned} \mathcal{L}(u, y, x; \lambda, \xi) \equiv \sum_i \left(\|y_i\|_2 - \lambda_i^\top (y_i - D_i u) + \frac{\beta_1}{2} \|y_i - D_i u\|_2^2 \right) \\ + \frac{\mu}{2}\|u - g\|_2^2 - \xi^\top (x - u) + \frac{\beta_2}{2}\|x - u\|_2^2, \end{aligned} \tag{2.8}$$

where $\beta_1, \beta_2 > 0$. Then one step iteration of ADMM reads

$$\begin{aligned} &\begin{pmatrix} y^{k+1} \\ x^{k+1} \end{pmatrix} \leftarrow \arg \min_{x \in \Omega, y} \mathcal{L}_{\mathcal{A}} \left(u^k, y, x; \lambda^k, \xi^k \right), \\ &u^{k+1} \leftarrow \arg \min_u \mathcal{L}_{\mathcal{A}} \left(u, y^{k+1}, x^{k+1}; \lambda^k, \xi^k \right), \\ &\begin{pmatrix} \lambda^{k+1} \\ \xi^{k+1} \end{pmatrix} \leftarrow \begin{pmatrix} \lambda^k - \beta_1 \left(y^{k+1} - D u^{k+1} \right) \\ \xi^k - \beta_2 \left(x^{k+1} - u^{k+1} \right) \end{pmatrix}. \end{aligned} \tag{2.9}$$

The (x, y)-subproblem can be solved in closed form

$$\begin{aligned} x^{k+1} &= \underset{x \in \Omega}{\operatorname{argmin}} \left\{ \left(\xi^k\right)^\top (x - u^k) + \frac{\beta_2}{2}\|x - u\|_2^2 \right\} = P_\Omega \left[u^k + \frac{\xi^k}{\beta_2} \right], \\ y_i^{k+1} &= \underset{y_i}{\operatorname{argmin}} \left(\|y_i\|_2 - \lambda_i^k \left(y_i - D_i u^k \right) + \frac{\beta_1}{2} \left\| y_i - D_i u^k \right\|_2^2 \right) \\ &= \max \left\{ \left\| D_i u^k + \frac{1}{\beta_1} \left(\lambda^k \right)_i \right\|_2 - \frac{1}{\beta_1}, 0 \right\} \frac{D_i u^k + \frac{1}{\beta_1} \left(\lambda^k \right)_i}{\left\| D_i u^k + \frac{1}{\beta_1} \left(\lambda^k \right)_i \right\|_2}, \quad i = 1, \ldots, n^2. \end{aligned}$$

The u-subproblem is a quadratic optimization problem which can be solved by FFT efficiently

$$\begin{aligned} u^{k+1} = \underset{u}{\operatorname{argmin}} \Big\{ &- \left(\lambda^k\right)^\top \left(y^{k+1} - Du \right) + \frac{\beta_1}{2} \left\| y^{k+1} - Du \right\|_2^2 + \frac{\mu}{2}\|u - g\|_2^2 \\ &- \left(\xi^k\right)^\top \left(x^{k+1} - u \right) + \frac{\beta_2}{2} \left\| x^{k+1} - u \right\|_2^2 \Big\} \\ = \left(D^\top D + \frac{\mu + \beta_2}{\beta_1} I \right)^{-1} &\left(D^\top \left(y^{k+1} - \frac{\lambda^k}{\beta_1} \right) + \frac{\mu}{\beta_1} g + \frac{\beta_2}{\beta_1} \left(x^{k+1} - \frac{\xi^k}{\beta_2} \right) \right). \end{aligned}$$

3. Convergence of the iterative algorithm

We will study the convergence of Algorithm 2.1 in this section. First, we recall the definition of the nonexpansive operator and asymptotically regular operator as in [22] and [3], respectively. Let $C \subset X$ be a convex closed subset of a Banach space X.

Definition 3.1 (Nonexpansive). *An operator $T : C \to X$ is nonexpansive if $\|T(x) - T(y)\| \leq \|x - y\|$ for any x, y in C.*

Definition 3.2 (Asymptotically regular). *$T : C \to C$ is asymptotically regular if for arbitrary x in C, $\lim_{n\to\infty} T^{n+1}x - T^n x = (I - T)(T^n x) = 0$.*

The convergence for the nonexpansive and asymptotically regular nonlinear operator is discussed in [3].

Proposition 3.1 ([3]). *If $T : C \to C$ is a nonexpansive asymptotically regular mapping and there exists a fixed point for T, then for any x in C, the sequence of successive approximations $\{T^n x\}$ is weakly convergent to a fixed point of T.*

We then rewrite Algorithm 2.1 in operator form. Let z and u be the solutions of problem (2.2) and (2.3), respectively (where we omit the sup-script k), then we define the operator R and S by $e^z = R(u)$ and $u = S(e^z)$. With the help the composed operator $T = SR$, the iteration for Algorithm 2.1 can reformulated by $u^{(k)} = SR(u^{(k-1)}) = T(u^{(k-1)})$. We will show that operator T satisfies all properties in Proposition 3.1.

Now we discuss the choice to the box constraint Ω. It has been discussed in [7] that imposing box constraints on TV denoising models can achieve more accurate solutions. A standard box constraint (for a normalized image) is $\Omega = \{u : 0 \leq u \leq 1\}$. To obtain the convergence of algorithm, we impose the box constraint by $\Omega = \{u : 0 \leq u \leq \min\{2f, 1\}\}$. This box constraint is for the technique reason, and has also been used for other similar nonconvex problem, see, e.g. [1]. To apply Proposition 3.1, we choose the convex set $C = \Omega$, and need to show the operator $T : \Omega \to \Omega$ is nonexpansive and asymptotically regular.

Lemma 3.1. *Operator T from Ω to Ω is nonexpansive.*

Proof. From definition $T = SR$, we only need to show

(1) Given any u and v in Ω, $\|R(u) - R(v)\| \leq \|u - v\|$.

(2) Given any z_1 and z_2, we have $\|S(e^{z_1}) - S(e^{z_2})\| \leq \|e^{z_1} - e^{z_2}\|$.

For claim (1): Let $e^z = R(u)$ and $e^y = R(v)$, then for each pixel i we have

$$\begin{aligned} &1 - [f]_i e^{-[z]_i} + 2\alpha_1 \left(e^{[z]_i} - [u]_i\right) e^{[z]_i} = 0, \\ &1 - [f]_i e^{-[y]_i} + 2\alpha_1 \left(e^{[y]_i} - [v]_i\right) e^{[y]_i} = 0. \end{aligned} \tag{3.1}$$

Since $[u]_i \le 2[f]_i$, then for any $[z]_i$ such that $e^{[z]_i} \ge 2[f]_i \ge [u]_i$, we have

$$1 - [f]_i e^{-[z]_i} + 2\alpha_1 \big(e^{[z]_i} - [u]_i\big) e^{[z]_i} > 1 - \frac{1}{2} > 0,$$

which implies that

$$e^{[z]_i} < 2[f]_i, \quad e^{[y]_i} < 2[f]_i. \tag{3.2}$$

From (3.1) we obtain that

$$\begin{aligned}
[u]_i &= e^{[z]_i} + \frac{1}{2\alpha_1}\left(e^{-[z]_i} - [f]_i e^{-2[z]_i}\right), \\
[v]_i &= e^{[y]_i} + \frac{1}{2\alpha_1}\left(e^{-[y]_i} - [f]_i e^{-2[y]_i}\right).
\end{aligned}$$

Simple computation yields that

$$\begin{aligned}
[u]_i - [v]_i &= e^{[z]_i} - e^{[y]_i} + \frac{1}{2\alpha_1}\left(e^{-[z]_i} - e^{-[y]_i} - [f]_i e^{-2[z]_i} + [f]_i e^{-2[y]_i}\right) \\
&= \big(e^{[z]_i} - e^{[y]_i}\big)\left(1 - \frac{1}{2\alpha_1}\frac{1}{e^{[z]_i}e^{[y]_i}} + \frac{[f]_i}{2\alpha_1}\frac{e^{[z]_i} + e^{[y]_i}}{e^{2[z]_i}e^{2[y]_i}}\right) \\
&= \big(e^{[z]_i} - e^{[y]_i}\big)\left(1 + \frac{1}{2\alpha_1}\frac{1}{e^{[z]_i}e^{[y]_i}}\left\{\frac{[f]_i}{e^{[z]_i}} + \frac{[f]_i}{e^{[y]_i}} - 1\right\}\right).
\end{aligned}$$

From (3.2) we obtain that

$$\big|[u]_i - [v]_i\big| > \big|e^{[z]_i} - e^{[y]_i}\big|$$

it implies $\|e^z - e^y\| \le \|u - v\|$, which finished the proof to claim (1).

For claim (2), we notice that problem (2.3) can be formulated as (by omitting subscript k)

$$u = \operatorname{argmin} \frac{1}{2}\|u - e^z\|^2 + \frac{\alpha_2}{2\alpha_1}\|u\|_{TV} + I_\Omega(u),$$

where I_Ω is an indicate function which is defined by

$$I_\Omega(u) = \begin{cases} 0, & u \in \Omega, \\ +\infty, & \text{otherwise.} \end{cases}$$

Then operator S is same as the prioximal operator prox_ϕ, where

$$\phi(u) = \frac{\alpha_2}{2\alpha_1}\|u\|_{TV} + I_\Omega(u).$$

Since the proximal operator is 1-Lipschitz operator, see, e.g., [6], we show the claim (2). Combining claims (1) and (2), we have that operator T is nonexpansive. $\square$

Next we study the asymptotical regularity of T.

Lemma 3.2. *For any initial guess $u^{(0)} \in \Omega$, T is asymptotically regular.*

Proof. Using the notation

$$\phi(u) = \frac{\alpha_2}{2\alpha_1}\|u\|_{TV} + I_\Omega(u),$$

we write the problem (2.3) as

$$u^{(k)} = \operatorname{argmin} \frac{1}{2}\|u - e^{z^{(k)}}\|^2 + \phi(u).$$

From the first order optimality condition, we have

$$e^{z^{(k)}} - u^{(k)} \in \partial\phi\big(u^{(k)}\big).$$

From the definition for the subderivative, we obtain that

$$\phi\big(u^{(k-1)}\big) - \phi\big(u^{(k)}\big) \geq \big(e^{z^{(k)}} - u^{(k)}\big) \cdot \big(u^{(k-1)} - u^{(k)}\big).$$

It implies that

$$\begin{aligned} &\frac{1}{2}\big\|u^{(k-1) - e^{z^{(k)}}}\big\| + \phi\big(u^{(k-1)}\big) \\ \geq &\frac{1}{2}\big\|u^{(k) - e^{z^{(k)}}}\big\| + \phi\big(u^{(k)}\big) + \frac{1}{2}\big\|u^{(k-1)} - u^{(k)}\big\|^2. \end{aligned}$$

Since $u^{(k)}$ and $u^{(k-1)}$ are in Ω, the above inequality is

$$\begin{aligned} &\alpha_1\big\|u^{(k-1) - e^{z^{(k)}}}\big\| + \alpha_2\big\|u^{(k-1)}\big\|_{TV} \\ \geq &\alpha_1\big\|u^{(k) - e^{z^{(k)}}}\big\| + \alpha_2\big\|u^{(k)}\big\|_{TV} + \alpha_1\big\|u^{(k-1)} - u^{(k)}\big\|^2. \end{aligned} \tag{3.3}$$

Recall (2.1) for the definition of $E(z,u)$ by

$$E(z,u) = \sum_{i=1}^{n^2}\Big([z]_i + [f]_i e^{-[z]_i}\Big) + \alpha_1\|u - e^z\|_2^2 + \alpha_2\|u\|_{TV},$$

then from (3.3) and (2.2), we have

$$E\big(z^{(k)}, u^{(k)}\big) + \alpha_1\big\|u^{(k-1)} - u^{(k)}\big\|^2 \leq E\big(z^{(k)}, u^{(k-1)}\big) \leq E\big(z^{(k-1)}, u^{(k-1)}\big).$$

Summing them up, we obtain that $\sum_{k=1}^{\infty}\|u^{(k)} - u^{(k-1)}\|_2^2$ is bounded, hence $\|u^{(k)} - u^{(k-1)}\|_2^2 \to 0$, as $k \to \infty$, i.e. $\lim_{n\to\infty}\|T^{k+1}u_0 - T^k u_0\| = 0$. Therefor operator T is asymptotically regular. $\square$

Lemma 3.3. *There exists a fixed point for T, i.e., the set $\{u|u = Tu\}$ is nonempty.*

Proof. If (z,u) is the global minimum point of $E(z,u)$, then u is a fixed point of T. Next we will show there exists a global minimizer of $E(z,u)$. Clearly E is continuous, then we need to show $E(z,u)$ is coercive. From the box constraint Ω for u, we only need to consider the case of $\|z\| \to +\infty$. For any given $[f]_i > 0$, the function

$$h(t) = t + [f]_i e^{-t} \geq \begin{cases} t, & t \geq 0, \\ \dfrac{[f]_i}{4}t^2 - \dfrac{1}{[f]_i}, & t < 0. \end{cases}$$

Hence $\|z\| \to +\infty$ implies that $E(z,u) \to +\infty$, which prove the coercivity of E. $\square$

Combining Lemmas 3.1-3.3 and Proposition 3.1, we have the following convergence result.

Theorem 3.1. *For arbitrary initial $u^{(0)}$, the sequence $\{u^{(k)}\}$ generated by Algorithm 2.1, i.e., $u^{(k)} = SR(u^{(k-1)})$ converges weakly to a fixed point of T.*

4. Numerical experiments

In this section we compare the proposed method with the other two methods: AA model [1] and HM model [18] for three tested images, see Fig. 1. Given the true image u and a restored image $\overline{u}$, we use the peak signal to noise ratio (PSNR) and the relative error to estimate the image quality.

$$PSNR(u,\overline{u}) = 10\log_{10}\left(\frac{\max\left(\max(u),\max(\overline{u})\right)^2}{\mid u - \overline{u}\mid^2}\right),$$

$$ReErr(u,\overline{u}) = \frac{\|u-\overline{u}\|_2^2}{\|u\|_2^2}.$$

The multiplicative noise follows Gamma distribution (1.1) with $K\theta = 1$ and we test three different noise levels: $K = 33$, $K = 13$, $K = 5$, respectively. We consider two

Figure 1: Original images, (a) Lena, (b) cameraman, and (c) shape.

different initial guesses of u in Algorithm 2.1, observed image f and the mean of f. Let the number of maximum iterations be 3000, and the stopping criteria be as

$$\frac{\|u^{(k+1)} - u^{(k)}\|_2}{\|u^k\|_2} < 10^{-4}.$$

For technique reason, we consider the box constraint $\Omega = \{u : 0 \leq u \leq \min\{1, 2f\}\}$ in Section 3. A more natural choice is $\Omega = \{u : 0 \leq u \leq 1\}$. We let $K = 30$ in Fig. 1(b) and compare the numerical results for two different box constraints. One can find them are very close, i.e., the $PSNR$ are 28.0728 and 28.0686 for two box constraints, respectively. In later computation, we will use $\Omega = \{u : 0 \leq u \leq 1\}$ for simplicity.

There are two hyper parameters α_1 and α_2 in the proposed model. When α_2 is fixed, the choice of α_1 does not affect the results, see Table 1 for $\alpha_2 = 0.2$ and $K = 35$.

Table 1: Different choices to parameter α_1.

α_1	20	15	10	5
ReErr	0.0725	0.0716	0.0716	0.0717
PSNR	28.4037	28.4739	28.4874	28.4273

We will choose $\alpha_1 = 5$ in all numerical tests except for $K = 5$ (we slightly change $\alpha_1 = 6$ in the large noise case to get a better result). The choice of α_2 is similar as parameters selection for TV denoise model, which can be determined by a lot of method, e.g., discrepancy principle [29]. The numerical results are shown in Tables 2-4. It can be found that the proposed model recovers a comparable results with AA model and HM model but with less CPU time and iteration steps. The noisy and recovered images can be found in Figs. 2-9, where Figs. 2, 4, 8 are the images degraded by different noise level, and Figs. 3, 5, 9 are the images restored by our method and HM method with different initial guess for u.

In Table 2, when the noise is small ($K = 33$), our method is superior to the other two in PSNR, time and iteration number. Our method is also stable for two different initialization, while AA model relies on the initialization.

Figure 2: Noisy images with $K = 33$.

Table 2: Restoration results with $K = 33$.

Images	Methods	$u^{(0)} = mean(f)$				$u^{(0)} = f$			
		ReErr	PSNR(db)	#Iter	Time(s)	ReErr	PSNR(db)	#Iter	Time(s)
(a)	Our model	0.0703	28.5047	27	9.77	0.0719	28.4020	21	7.28
	AA model	0.1003	25.6286	726	24	0.0706	28.6831	436	12.53
	HM model	0.0706	28.4479	192	15.52	0.0708	28.3664	115	16.63
(b)	Our model	0.0744	28.1057	24	9.13	0.0758	28.1196	20	9.28
	AA model	0.0998	25.5335	726	20.47	0.0755	28.0180	489	14.99
	HM model	0.0767	27.8963	193	16.55	0.0763	27.9684	111	10.03
(c)	Our model	0.0371	31.9875	53	5.84	0.0386	31.8012	24	3.48
	AA model	0.2466	15.1182	3000	19.3941	0.2459	15.1463	3000	19.3784
	HM model	0.0402	31.8308	196	7.16	0.0413	32.0106	198	7.09

In Tables 3-4, for the moderate noise ($K = 13$) and large noise ($K = 5$), our method is comparable with the other two in PSNR, and superior in time. In Fig. 5, we can see that our method can preserve textures and details well. To see the details more clearly, we test $K = 15$ in Fig. 6 and enlarge part of the image to view the details of the restored image by our method and HM method. Local details such as the mouth of the cameraman and the pillar of the building are better restored with our method

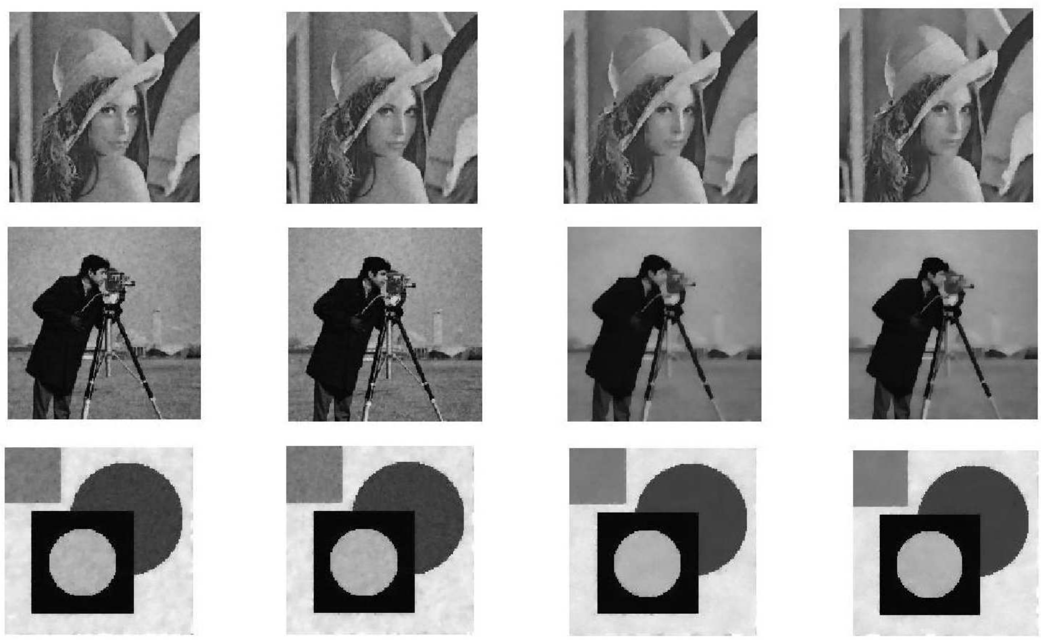

Figure 3: Images restored by our method and HM method with $K = 33$. First two columns are our method, the last two columns are HM method. Initial guess of u: column 1,3 are observed image while column 2,4 are the mean of observed image. $\alpha_1 = 5$, $\alpha_2 = 0.2$

Figure 4: Noisy images with $K = 13$.

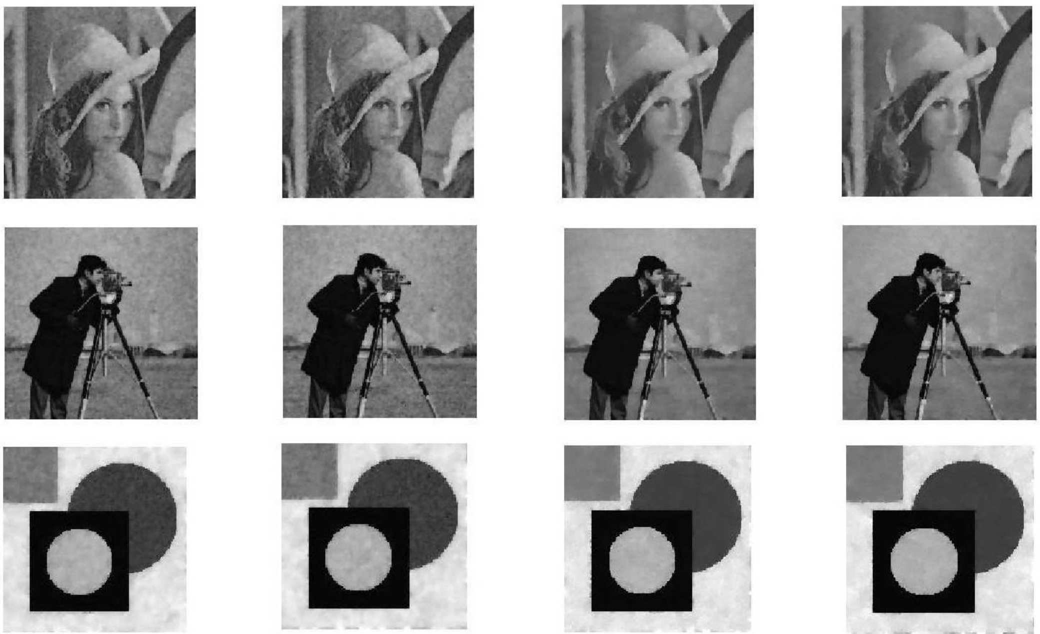

Figure 5: Images restored by our method and HM method with $K = 13$. First two columns are our method, the last two columns are HM method. Initial guess of u: column 1,3 are observed image while column 2,4 are the mean of observed image.$\alpha_1 = 5$, $\alpha_2 = 0.4$.

Figure 6: Images restored by our method (left) and HM method (right) with K=15 and the middle two columns are local enlargement.

Table 3: Restoration results with $K = 13$.

Images	Methods	$u^{(0)} = mean(f)$				$u^{(0)} = f$			
		ReErr	PSNR(db)	#Iter	Time(s)	ReErr	PSNR(db)	#Iter	Time(s)
(a)	Our model	0.0903	26.5433	24	10.41	0.0901	26.5596	33	13.94
	AA model	0.1080	24.9893	741	20.8890	0.0909	26.4985	718	21.29
	HM model	0.1004	25.4771	176	19.08	0.0922	25.5423	153	19.14
(b)	Our model	0.0955	25.9181	24	11.80	0.0961	25.8605	24	9.91
	AA model	0.0908	26.3536	3000	92.09	0.0908	26.3509	3000	86.41
	HM model	0.1001	25.5780	197	19.03	0.1005	25.5127	163	18.92
(c)	Our model	0.0580	27.5966	27	5.13	0.0587	27.4908	22	5.27
	AA model	0.2489	15.0025	3000	19.4495	0.2471	15.1058	3000	20.2544
	HM model	0.0671	28.6940	200	7.72	0.0680	27.9683	153	6.92

Table 4: Restoration results with $K = 5$.

Images	Methods	$u^{(0)} = mean(f)$				$u^{(0)} = f$			
		ReErr	PSNR(db)	#Iter	Time(s)	ReErr	PSNR(db)	#Iter	Time(s)
(a)	Our model	0.1123	24.6848	53	16.53	0.1234	24.1731	27	12.96
	AA model	0.1577	21.7011	2445	69.77	0.1726	20.9538	1055	30.53
	HM model	0.1216	24.4320	187	17.53	0.1176	24.1783	185	17.51
(b)	Our model	0.1234	23.6855	35	12.75	0.1281	23.2025	21	10.19
	AA model	0.1584	21.7303	3000	87.11	0.1636	21.5035	3000	87.24
	HM model	0.1241	23.6398	166	14.22	0.1245	23.5762	162	14.20
(c)	Our model	0.0748	25.5368	41	10.45	0.0806	25.3146	37	9.39
	AA model	0.2583	14.7390	3000	21.2425	0.2624	14.5658	3000	20.2399
	HM model	0.0931	26.7822	290	11.41	0.0963	26.6074	272	11.2

since we take TV regularization in the original image domain in our method, while HM takes regularization in the logarithmic domain of image which tend to oversmooth. To illustrate the advantages of our method in preserving details, we also compared with DZ model [10] in Fig. 7 with $K = 10$. DZ model is based on the statistical property of the noise, and a quadratic penalty function technique is utilized in order to obtain a strictly convex model under mild condition. But when K is small, the quadratic penalty can not fit the real noise well which may affect the restored results.

5. Conclusion

In this paper, we propose a multiplicative noise removal model and take TV regularization directly in the image domain, which preserves more details of images. An alternating iterative minimize algorithm is used to solve the minimization problem and convergence is provided under mildly condition. Several numerical examples with different noise levels are given to indicate the efficient of the proposed model.

Figure 7: Images restored by our method, HM method, and DZ method with $K = 10$.

Figure 8: Noisy images with $K = 5$.

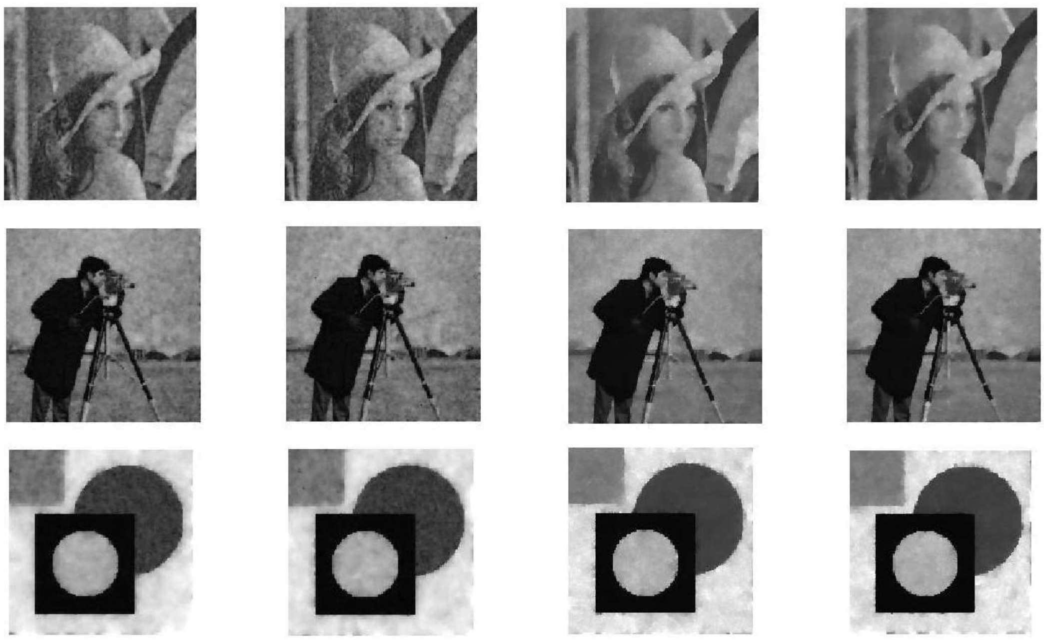

Figure 9: Images restored by our method and HM method with $K = 5$. First two columns are our method, the last two columns are HM method. Initial guess of u: column 1,3 are observed image while column 2,4 are the mean of observed image. $\alpha_1 = 6$, $\alpha_2 = 0.85$.

Acknowledgements

The authors would like to thank the anonymous referees for their useful suggestions that helped to improve the manuscript. The work of Xiliang Lu is partially supported by the National Key Research and Development Program of China (No. 2020YFA0714200), the National Science Foundation of China (No. 11871385) and by the Open Research Fund of KLATASDS2005. The numerical calculations in this paper have been done on the supercomputing system in the Supercomputing Center of Wuhan University.

References

[1] G. AUBERT AND J. AUJOL, *A variational approach to removing multiplicative noise*, SIAM J. Appl. Math. 68 (2008), 925–946.

[2] S. P. AWATE AND R. T. WHITAKER, *Nonparametric neighborhood statistics for mri denoising*, in: *Information Processing in Medical Imaging*, Springer, (2005), 677–688.

[3] F. BROWDER AND W. PETRYSHYN, *The solution by iteration of nonlinear functional equations in banach spaces*, Bull. Amer. Math. Soc. 72 (1966), 571–575.

[4] A. CHAMBOLLE, *An algorithm for total variation minimization and applications*, J. Math. Imaging Vision 20 (2004), 89–97.

[5] A. CHAMBOLLE AND T. POCK, *A first-order primal-dual algorithm for convex problems with applications to imaging*, J. Math. Imaging Vision 40 (2010), 120–145.

[6] A. CHAMBOLLE AND T. POCK, *An introduction to continuous optimization for imaging*, Acta Numerica 25 (2016), 161–319.

[7] R. CHAN, M. TAO, AND X. YUAN, *Constrained total variation deblurring models and fast algorithms based on alternating direction method of multipliers*, SIAM J. Imaging Sci. 6 (2013), 680–697.

[8] L. CHEN, X. LIU, X. WANG, AND P. ZHU, *Multiplicative noise removal via nonlocal similarity-based sparse representation*, J. Math. Imaging Vision 54 (2015), 199–215.

[9] P. CHEN, J. HUANG, AND X. ZHANG, *A primal-dual fixed point algorithm for convex separable minimization with applications to image restoration*, Inverse Problems 29 (2013), 025011.

[10] Y. DONG AND T. ZENG, *A convex variational model for restoring blurred images with multiplicative noise*, SIAM J. Imaging Sci. 6 (2013), 1598–1625.

[11] A. EL-HAMIDI, M. MÉNARD, M. LUGIEZ, AND C. GHANNAM, *Weighted and extended total variation for image restoration and decomposition*, Pattern Recognit. 43 (2010), 1564–1576.

[12] E. ESSER, *Applications of Lagrangian-based alternating direction methods and connections to split bregman*, CAM Rep, (2010).

[13] F. FANG, F. LI, AND T. ZENG, *Single image dehazing and denoising: A fast variational approach*, SIAM J. Imaging Sci. 7 (2014), 969–996.

[14] T. GOLDSTEIN AND S. OSHER, *The split bregman algorithm for l1-regularized problems*, SIAM J. Imaging Sci. 2 (2009), 323–343.

[15] R. GRIESSE AND D. A. LORENZ, *A semismooth Newton method for Tikhonov functionals with sparsity constraints*, Inverse Problems 24 (2008), 035007.

[16] A. HADDAD AND Y. MEYER, *An improvement of Rudin-Osher-Fatemi model*, Appl. Comput. Harmon. Anal. 22 (2007), 319–334.

[17] J. Huang and X. Yang, *Fast reduction of speckle noise in real ultrasound images*, Signal Process. 93 (2013), 684–694.

[18] Y. Huang, M. Ng, and Y.-W. Wen, *A new total variation method for multiplicative noise removal*, SIAM J. Imaging Sci. 2 (2009), 20–40.

[19] Z. Jian, C. Zheng-wen, and Z. Mingquan, *Sar image denoising based on wavelet-fractal analysis*, J. Syst. Eng. Electron. 18 (2007), 45–48.

[20] F. Li, M. Ng, and C. Shen, *Multiplicative noise removal with spatially varying regularization parameters*, SIAM J. Imaging Sci. 3 (2010), 1–20.

[21] Y. Lou, T. Zeng, S. Osher, and J. Xin, *A weighted difference of anisotropic and isotropic total variation model for image processing*, SIAM J. Imaging Sci. 8 (2015), 1798–1823.

[22] Z. Opial, *Weak convergence of the sequence of successive approximations for nonexpansive mappings*, Bulletin of the American Mathematical Society, 73 (1967), 591–597.

[23] L. Rudin, P. L. Lions, and S. Osher, *Multiplicative denoising and deblurring: Theory and algorithms* in: *Geometric level set methods in imaging, vision, and graphics*, Springer, (2003), 103–119.

[24] L. Rudin, S. Osher, and E. Fatemi, *Nonlinear total variation based noise removal algorithms*, Phys. D 60 (1992), 259–268.

[25] J. Shi and S. Osher, *A nonlinear inverse scale space method for a convex multiplicative noise model*, SIAM J. Imaging Sci. 1 (2008), 294–321.

[26] G. Steidl and T. Teuber, *Removing multiplicative noise by Douglas-Rachford splitting methods*, J. Math. Imaging Vision 36 (2009), 168–184.

[27] W. Yin, D. Goldfarb, and S. Osher, *A comparison of three total variation based texture extraction models*, J. Vis. Commun. Image Represent. 18 (2007), 240–252.

[28] S. Yun and H. Woo, *A new multiplicative denoising variational model based on mth root transformation*, IEEE Trans. Image Process. 21 (2012), 2523–2533.

[29] R. Zanella, P. Boccacci, L. Zanni, and M. Bertero, *Efficient gradient projection methods for edge-preserving removal of poisson noise*, Inverse Problems 25 (2013), 045010.

[30] X.-L. Zhao, F. Wang, and M. Ng, *A new convex optimization model for multiplicative noise and blur removal*, SIAM J. Imaging Sci. 7 (2014), 456–475.